



HAL
open science

Biomechanical analysis of the correlation between mid-shaft atypical femoral fracture (AFF) and axial varus deformation

Mathieu Severyns, Dalila Belaid, Kevin Aubert, Ali Bouchoucha, Arnaud Germaneau, Tanguy Vendevre

► **To cite this version:**

Mathieu Severyns, Dalila Belaid, Kevin Aubert, Ali Bouchoucha, Arnaud Germaneau, et al.. Biomechanical analysis of the correlation between mid-shaft atypical femoral fracture (AFF) and axial varus deformation. *Journal of Orthopaedic Surgery and Research*, 2022, 17 (1), pp.165. 10.1186/s13018-022-03060-1 . hal-03844177

HAL Id: hal-03844177

<https://hal.science/hal-03844177v1>

Submitted on 9 Oct 2023

HAL is a multi-disciplinary open access archive for the deposit and dissemination of scientific research documents, whether they are published or not. The documents may come from teaching and research institutions in France or abroad, or from public or private research centers.


L'archive ouverte pluridisciplinaire **HAL**, est destinée au dépôt et à la diffusion de documents scientifiques de niveau recherche, publiés ou non, émanant des établissements d'enseignement et de recherche français ou étrangers, des laboratoires publics ou privés.

RESEARCH ARTICLE

Open Access



Biomechanical analysis of the correlation between mid-shaft atypical femoral fracture (AFF) and axial varus deformation

Mathieu Severyns^{1,2*} , Dalila Belaid^{2,3}, Kevin Aubert², Ali Bouchoucha³, Arnaud Germaneau² and Tanguy Vendevre²

Abstract

Background: Atypical femoral fractures (AFF) are diaphyseal fractures of the elderly that occur at the end of a minor trauma. The objective of this biomechanical study, using finite element modelling, was to evaluate the variations of the femoral diaphysis fracture indicator according to the variations of the mechanical axis of the lower limb, which can explain all the different atypical fracture types identified in the literature.

Methods: In order to measure variations in stress and risk factors for fracture of the femoral diaphysis, the distal end of the femur was constrained in all degrees of freedom. An axial compression load was applied to the femoral head to digitally simulate the bipodal support configuration in neutral position as well as in different axial positions in varus/valgus ($-10^{\circ}/10^{\circ}$).

Results: The maximum stress value of Von Mises was twice as high (17.96 ± 4.87 MPa) at a varus angle of -10° as in the neutral position. The fracture risk indicator of the femoral diaphysis varies proportionally with the absolute value of the steering angle. However, the largest simulated varus deformation (-10°) found a higher risk of diaphysis fracture indicator than in valgus (10°).

Conclusions: Variations in the mechanical axis of the lower limb influence the stress distribution at the femur diaphysis and consequently increase the risk of AFF. The axial deformation in varus is particularly at risk of AFF. The combination of axial deformation stresses and bone fragility consequently contribute to the creation of an environment favorable to the development of AFF.

Trial registration: 'retrospectively registered'.

Keywords: Atypical femoral fracture, Finite elements, Fracture risk indicator

Introduction

Atypical femoral fractures (AFF) are diaphyseal fractures of the elderly that occur as a result of minor trauma and may extend from the small trochanter to the supra-condylar metaphysis-diaphyseal junction

[1]. Strict diagnostic criteria have recently been developed by the American Society for Bone and Mineral Research (ASBMR) [2]. Four of the five major criteria must be met to make the diagnosis: (1) Minor trauma such as a fall from a height or absence of identified trauma, (2) Oblique or transverse fracture involving the external cortical, (3) Complete quadri-cortical fracture with a medial scale or incomplete fracture of interest to the lateral cortical, (4) Small or non-comminuted fracture, and (5) Localized thinning of the periosteum

*Correspondence: mathieu.severyns@hotmail.fr

¹ Department of Orthopaedic Surgery and Traumatology, Hôpital Pierre Zobda Quitman, University Hospital, 97261 Fort-de-France Cedex, Martinique, France

Full list of author information is available at the end of the article



or endostus of the external cortical. The concepts of iatrogenia (biphosphonates, glucocorticoids, proton pump inhibitors [3–5]) or comorbidities (rheumatoid arthritis, chronic kidney failure [6, 7]) are now reduced to minor criteria. Indeed, several scientific studies [8–11] have supported the mechanical theory that these atypical fractures are linked to an abnormal distribution of stresses on the lateral cortical area of the femur. Two major types of AFF now appear to be emerging: medial-diaphyseal fatigue fracture on curved femur and sub-trochanteric fracture [12]. The hypothesis of this work was that the higher the axial varus deformation of the lower limb the higher probability of AFF occurring. The objective of this biomechanical study, using finite element modelling, was therefore to evaluate the variations of the femoral diaphysis fracture indicator according to the variations of the mechanical axis of the lower limb, which can explain all the different atypical fracture types identified in the literature.

Table 1 Epidemiological and radiographic characteristics of whole femurs modelled as finite elements

Femur subject	AA	BB	CC	DD	EE
Age (year)	73	71	88	65	60
Gender	M	M	M	F	F
Side	R	L	R	R	L
Length (mm)	437.77	444.44	390.81	356.36	384.38
Neck-shaft angle (deg)	128.41	130.93	134.02	125.13	123.42
Hip-knee shaft angle (deg)	5.46	4.34	5.24	7.27	6.38

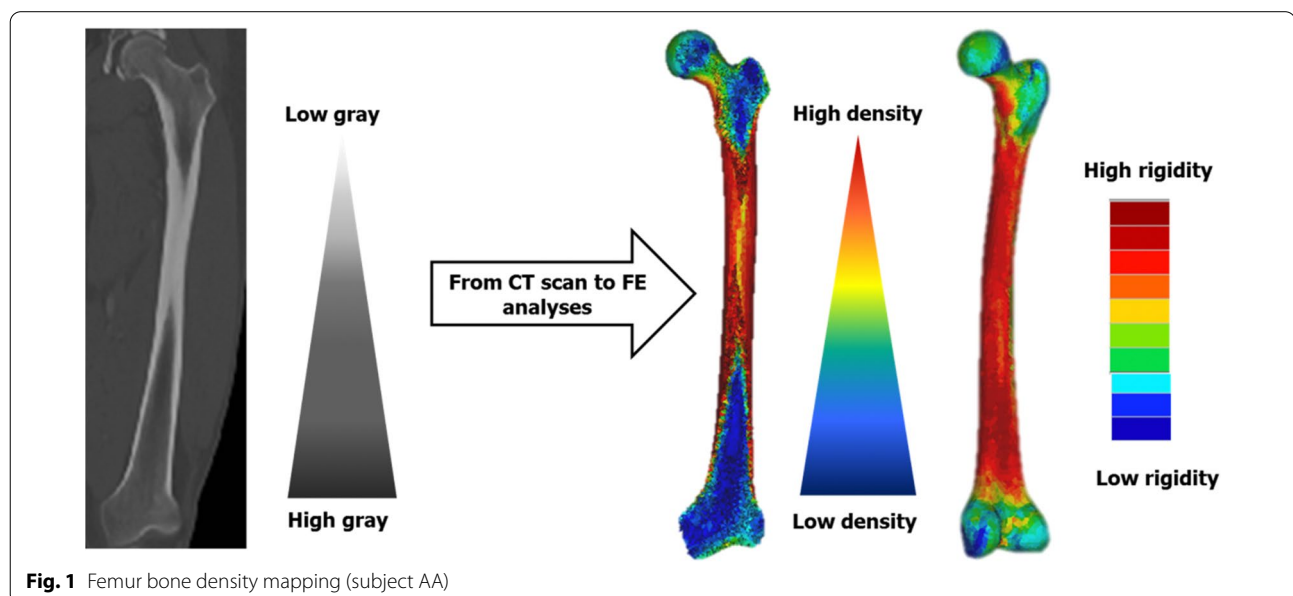
Methods

The analysis of load distribution and the effect of lower limb alignment was made possible by finite element modelling constructed from whole human femur CT scans ($n=5$). The epidemiological and radiological characteristics of patients are summarized in Table 1.

Finite element modeling (FE)

The methodology used to generate the numerical models was to reconstruct the entire femur from the CT scan acquisition. The X-ray scan parameters for the samples were set to 120 kVp, 100 mAs, with 0.75 mm cross-sections and an image matrix of 512×512 pixels with a pixel size of 0.434 mm. Volume image segmentation and geometric model were performed using 3D SLICER software (Version 4.11, Kitware, France). To perform finite element modeling, the resulting model was imported and analyzed using Ansys® Workbench software (Version 2020R2, Ansys Inc, United States). Bone segment geometry was discretized using ten-node tetrahedral element (C3D10), and mesh sensitivity was analyzed for elements of different sizes, as recommended in the literature [10, 13, 14].

The model elasticity modulus have been assigned element by element. Bone is considered heterogeneous and isotropic. For all models, a Poisson coefficient of 0.3 was assigned [15]. The grayscale values from the CT scan data (Fig. 1) express the Hounsfield (HU) units that identify bone density from the relationship (1) below with ρ_{QCT} as peripheric quantitative computed tomography [16]:



$$\rho_{QCT} \left(\text{g/cm}^3 \right) = 0.007764 \times \text{HU} - 0.056148 \quad (1)$$

In this work, the Young modulus of cortical and cancellous bones [17] allocated to each element was determined from the relationships below:

$$\rho_{\text{ash}} \left(\text{g/cm}^3 \right) = 0.877 \times \rho_{QCT} + 0.0789 \quad (2)$$

$$\rho_{\text{app}} \left(\text{g/cm}^3 \right) = \rho_{\text{ash}} / 0.6 \quad (3)$$

$$E \text{ (MPa)} = 6850 \times \rho_{\text{app}}^{1.49} \quad (4)$$

with ρ_{ash} as ash density, ρ_{app} as apparence density and E as elasticity module.

Alignment axes, loading and boundary conditions

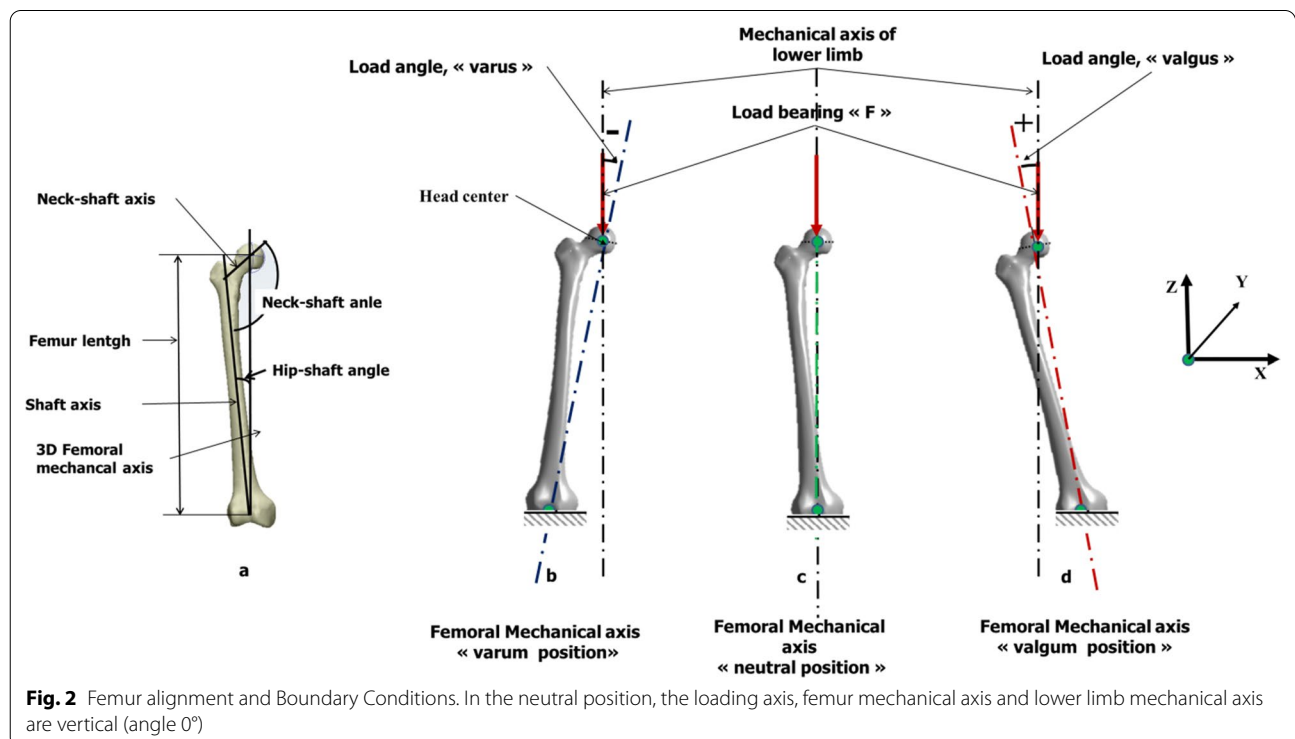
To determine the impact of lower limb alignment on stress amplitude and fracture risk factor, a load protocol corresponding to the standing position on both legs was modelled. In this scenario, in order to simulate the misalignment of the femur, it was necessary to identify the mechanical axes or loading axes. Reconstruction CT images were used to measure alignment [18]. The mechanical axis of the femur was considered a line connecting the center of the femur head and the center of the knee. In

order to measure the resistance of the femur, the distal end of the femur was constrained in all degrees of freedom. An axial compression load corresponding to an average weight of 70 kg (686 N) was applied to the center of the femoral head in neutral position as well as in varus/valgus position by rotating the femur around the center of the femoral head clockwise or counterclockwise in relation to the frontal plane (Fig. 2).

Post-treatments

Although the fracture force prediction and fracture site were based on the criteria of the maximum principal stress fracture theory, the fracture of a certain element has been defined as occurring when the maximum stress of the element exceeds its elastic limit. The atypical diaphyseal femur fracture risk indicator (FRI) was used for all load configurations, elucidating the effect of the anatomical variations of the femurs, their material properties and the mechanism of these fractures. The risk indicator for tensile fracture (TFRI) and femoral diaphysis compression (CFRI) was the ratio of ultimate (maximum) bone stress to limit stress and can be expressed as follows:

$$\text{CFRI} = \frac{\sigma_{\text{min,ppal}}^C}{\sigma_{\text{y,ppl}}^C} \quad (5)$$



$$TFRI = \frac{\sigma_{max,ppal}^T}{\sigma_{y,ppal}^T} \tag{6}$$

where $\sigma_{y,ppal}^C$ and $\sigma_{y,ppal}^T$ are respectively the stress limits in compressive and tensile strength; $\sigma_{max,ppal}^T$ and $\sigma_{min,ppal}^C$ are respectively the maximum and minimum main stresses.

After each load step, elements with the principal stress (σ_{ppal}) exceeding the yield stress ($\sigma_{y,ppal}$) were “failed” by assigning a very small Young’s modulus (1 MPa). The relationships used between $\sigma_{y,ppal}$ and ρ_{app} proposed by (Kheirollahi, et al.) [19] were stated as:

$$\sigma_y = 116\rho_{ash}^{2.03} \text{ (MPa)} \tag{7}$$

Results

The alignment of the lower limb influences the distribution of stresses in the femoral diaphysis in a bipodal load configuration. Deformation due to axial alignment variations also affects the risk of fracture.

Stress distribution

Figure 3 shows the variation in von Mises equivalent stress for all subjects. The mean maximum stress value of von Mises was 9.53 MPa (SD=2.52 MPa) for angle $0^\circ \pm$ while the mean maximum stress value of von Mises was 1.63 times higher (15.47 MPa, SD=5.68 MPa) for

angle 10° (valgus) and the stress value almost twice (17.96 MPa, SD=4.87 MPa) higher for the angle -10° (Table 2). There is also a clear increase in stress during varus deformation.

Figure 4 shows stress distribution in the diaphysis region. The highest absolute stress value is located at 10° and -10° angles and decreases as the angle approaches 0° (Table 3). Under the same load, (Table 3). Under the same load, and in the varus direction configuration, maximum main stress was localized at the lateral cortical femoral diaphysis, the minimum stress being localized at the medial cortical. On the contrary, under valgus stress, maximum main stress was localized at the antero-medial cortical level of the femoral diaphysis, minimum stress being localized at the lateral cortical. In addition, maximum stress was localized to the proximal diaphysis region in the neutral position and changed the localization to the distal diaphysis region at the valgus or varus angles. The stress values at the level of the femoral diaphysis evolved by varying the angle of varus or valgus.

Risk of atypical femoral fracture

To study the effect of misalignment on the risk of femur fracture, fracture indicators and tensile and compressive stress limits for the proximal femur and diaphysis were calculated separately. In all cases, the FRI based on the main stress criterion were calculated for the femur diaphysis in standing position, taking into account the

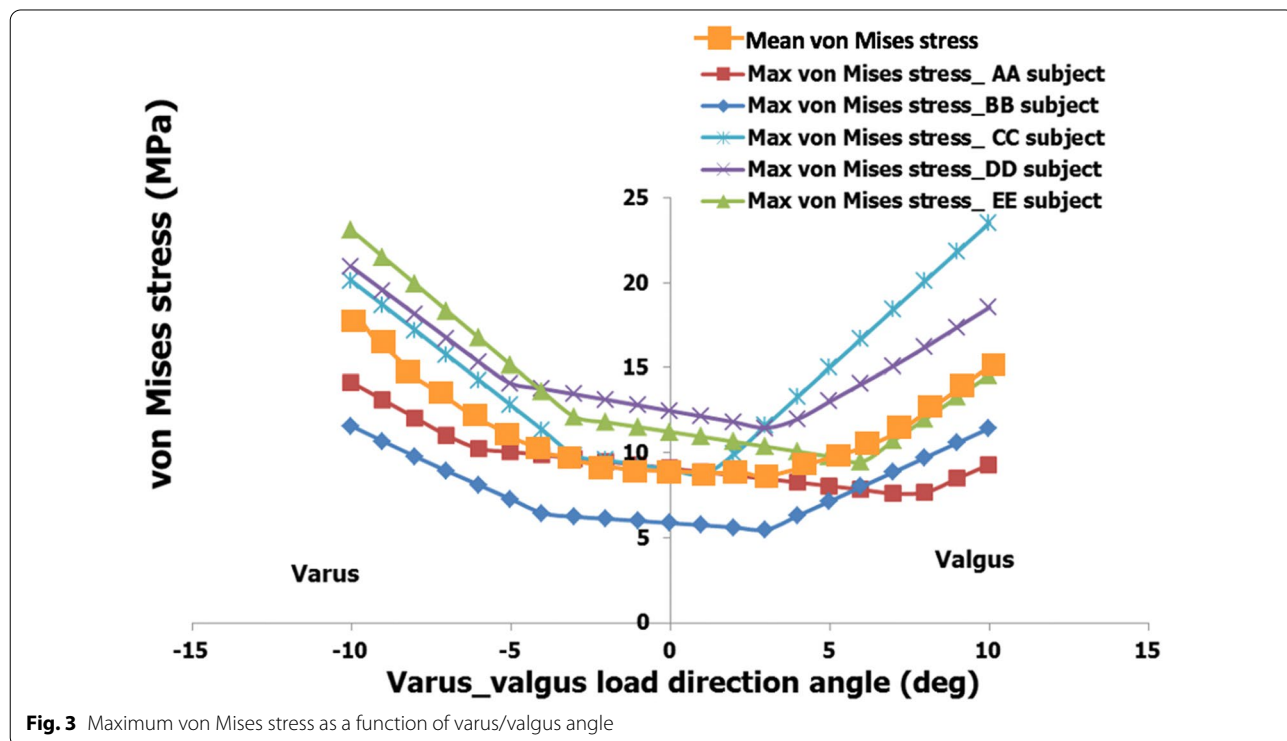


Fig. 3 Maximum von Mises stress as a function of varus/valgus angle

Table 2 The von Mises (MPa), (whole femur) maximum stress averages in all varus/valgus loads for the five subjects

		Maximum von Stress Bets (MPa)																				
Angle(deg)		-10	-9	-8	-7	-6	-5	-4	-3	-2	-1	0	1	2	3	4	5	6	7	8	9	10
Range		11.57–23.06	10.67–21.49	9.77–19.91	8.92–18.32	8.098–16.73	7.27–15.14	6.444–13.76	6.23–13.44	6.115–13.12	5.99–12.79	5.86–12.47	5.74–12.13	5.61–11.80	5.48–11.61	6.30–13.31	7.15–15.02	7.83–16.72	7.61–18.42	7.67–20.12	8.49–21.81	9.31–23.50
Average		17.96	16.69	15.41	14.14	12.93	11.87	10.99	10.26	10.02	9.78	9.53	9.29	9.33	9.48	9.99	10.60	11.22	12.15	13.15	14.31	15.47
SD		4.87	4.58	4.30	3.99	3.62	3.20	3.02	2.75	2.67	2.60	2.52	2.45	2.37	2.56	2.81	3.33	3.97	4.51	5.03	5.35	5.68

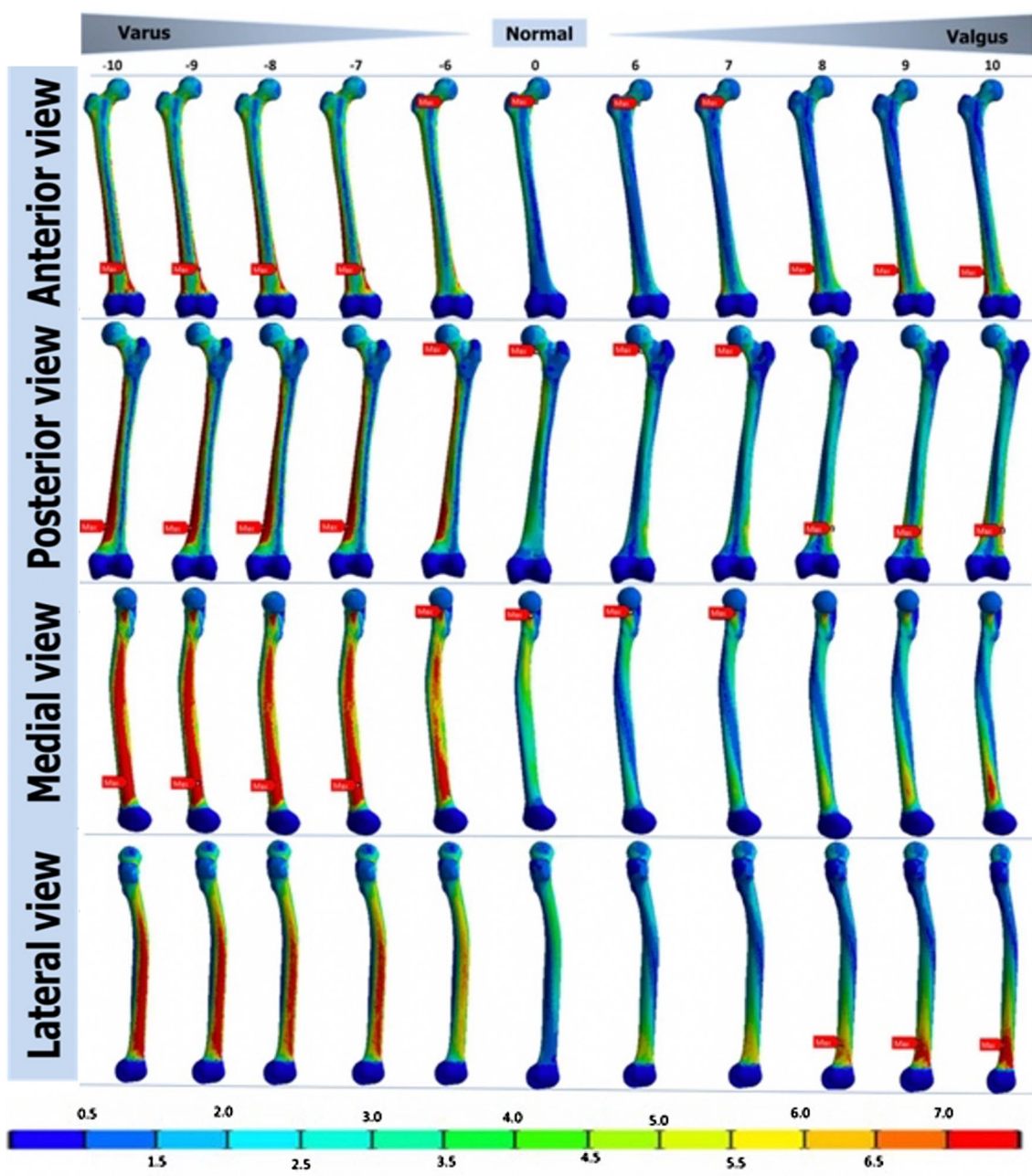


Fig. 4 Maximum von Mises stresses of the diaphyseal area for the subject AA. Valgus/varus angles: between -10° and -6° for valgus, between 6° and 10° for varus

inclination or direction of the load. The calculated FRI are shown in Fig. 5.

Increased risk indicator of diaphysis fracture was observed for maximum varus and valgus deformations. The FRI fracture risk indicator of the femoral diaphysis varies proportionally with the absolute value of the steering angle (Table 4). However, the largest varus

deformation simulated (-10°) found a higher risk of diaphysis fracture indicator than in valgus (10°).

The decrease in varus from -10° to 0° decreased the mean value of the compression fracture risk indicator from 0.131 (SD=0.036) to 0.051 (SD=0.008) respectively, and from 0.122 (SD=0.031) to 0.043 (SD=0.010).

Table 3 Means of the main strains of the femoral diaphysis in varus/valgus for the five subjects

Main stress (MPa)		-10	-9	-8	-7	-6	-5	-4	-3	-2	-1	0	1	2	3	4	5	6	7	8	9	10
<i>Minimum</i>																						
Range(abs)		23.17–11.73	21.59–10.82	20.03–9.911	18.46–8.993	16.88–8.132	15.30–7.301	13.71–6.468	12.12–5.869	10.64–5.576	9.318–5.281	8.457–4.987	8.438–4.821	9.412–4.690	10.40–4.569	11.39–4.496	12.38–5.188	13.37–5.907	14.36–6.759	15.44–7.609	16.56–8.457	17.67–9.303
Average		-18.29	-16.99	-15.69	-14.39	-13.10	-11.81	-10.51	-9.27	-8.29	-7.44	-6.81	-6.92	-7.44	-8.06	-8.79	-9.87	-11.04	-12.22	-13.41	-14.62	-15.82
SD		5.01	4.70	4.41	4.12	3.81	3.49	3.17	2.76	2.19	1.73	1.56	1.64	2.09	2.71	3.38	3.76	4.03	4.30	4.59	4.89	5.20
<i>Maximum</i>																						
Rank		9.72–19.65	8.94–18.23	7.92–16.80	7.32–15.37	6.71–13.94	6.10–12.5	5.58–11.05	5.07–9.608	4.37–8.409	3.84–7.311	3.32–6.567	2.81–5.821	2.42–5.209	2.82–4.755	2.73–4.299	2.69–4.884	3.69–6.271	4.54–7.656	5.36–9.039	6.21–10.53	7.11–12.16
Average		14.01	12.77	11.54	10.52	9.58	8.67	7.77	6.89	6.07	5.36	4.77	4.28	3.85	3.60	3.44	3.88	5.10	6.35	7.61	8.87	10.13
SD		4.73	4.56	4.40	4.08	3.67	3.27	2.85	2.43	2.06	1.76	1.52	1.36	1.23	0.87	0.61	0.81	1.03	1.26	1.50	1.75	2.01

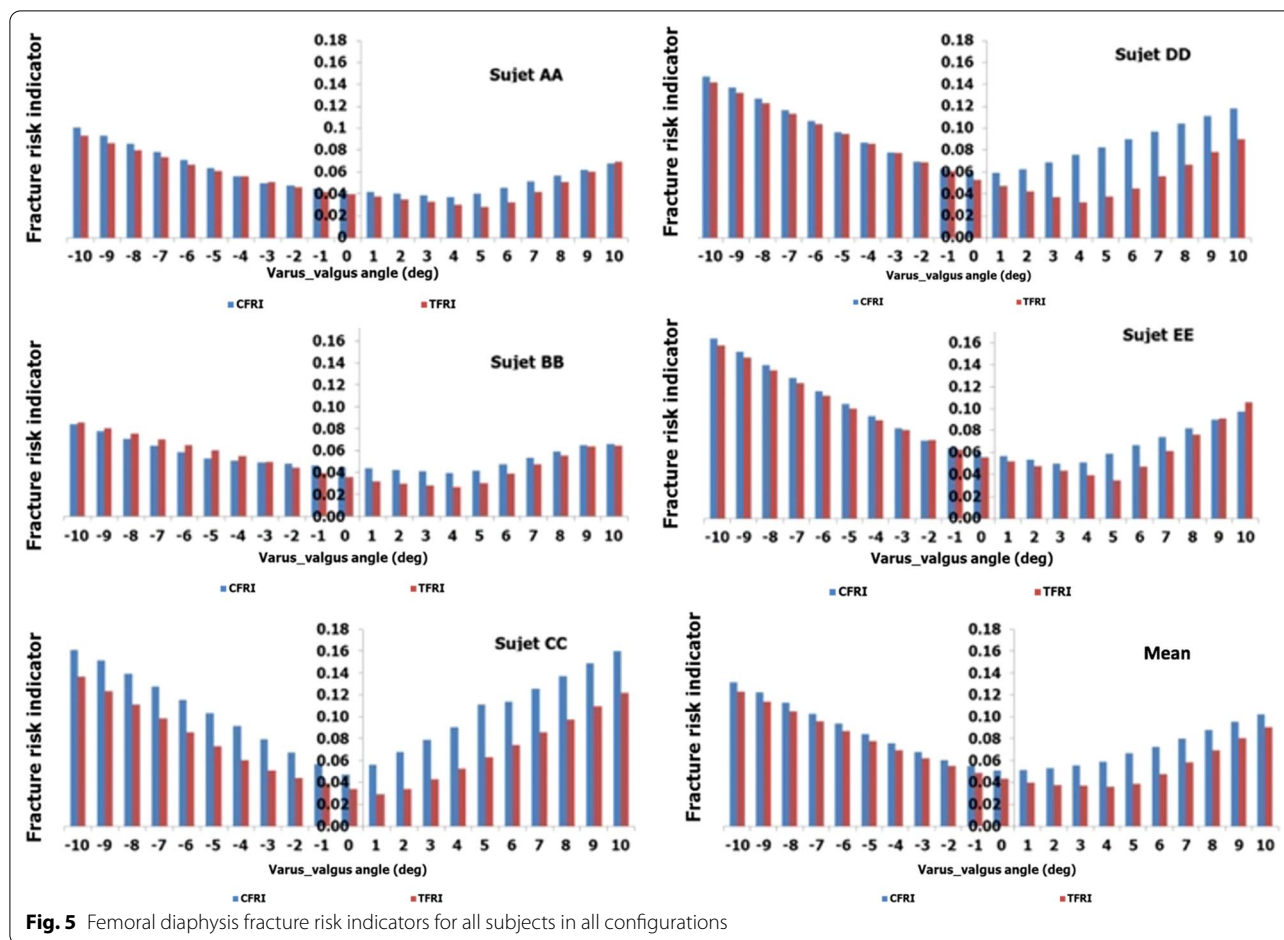


Fig. 5 Femoral diaphysis fracture risk indicators for all subjects in all configurations

The increase in valgus deformation from 0° to 10° increased the mean value of the compression fracture risk indicator and the mean value of the traction fracture risk indicator respectively from 0.051 (SD=0.008) to 0.101 (SD=0.039), and from 0.043 (SD=0.010) to 0.090 (SD=0.024).

Discussion

Axial deformation in varus of the lower limb, all causes combined, presented a higher risk indicator of femoral diaphysis fracture than in valgus. This means that varus alignment could play a major role in AFF pathophysiology. The diaphyseal fracture risk indicators have the highest values for extreme axial deformation (-10°/10°). This shows a strong correlation between AFF risk and the mechanical axis in varus/valgus.

In the literature, some studies have associated diaphyseal femoral stresses with axial deformities due to femoral curvilinear (primary or secondary) malformations. Oh et al. [9] demonstrated using a tomography-based finite element method that patients with arched femoral diaphysis had greater stresses on the anterolateral surface

of the diaphysis. Sasaki et al. [8] compared the femoral curvature of nine elderly patients treated for low energy diaphyseal femoral fractures with those of 24 controls without fractures. They reported that femoral curvature was significantly higher in patients with AFF compared to the control group, suggesting that an increase in femoral curvature could be a causal factor of AFF. For the same purpose, Morin et al. studied femoral geometric parameters using EOS imaging of 16 Caucasian women with AFF [20]. Their analysis showed that these patients had a more laterally curved femur of -3.2° (SD=3.4) versus -0.8° (SD=1.9) for the control group. Our study evaluated the femoral stress distribution as well as the risk of AFF exerted on a member in varus, whatever its origin: femoral, tibial, or femoral-tibial. The observed results highlight the importance of considering axial deformation as a whole, and not only on the curvilinear character of the femur.

Regarding the location of the fracture, for Oh et al. [9] they appeared to be full-blown fatigue fractures of the mid-shaft diaphyseal fractures on the curved femur. The location of the atypical fracture could then be determined

Table 4 Femoral diaphysis fracture risk indicator averages in varus/valgus for all five subjects

FRI risk indicator invoice		-10	-9	-8	-7	-6	-5	-4	-3	-2	-1	0	1	2	3	4	5	6	7	8	9	10
<i>Compressive</i>																						
Range		0.084–0.163	0.077–0.152	0.070–0.140	0.064–0.128	0.058–0.115	0.052–0.104	0.050–0.093	0.049–0.082	0.047–0.071	0.045–0.063	0.043–0.060	0.041–0.059	0.040–0.067	0.038–0.079	0.036–0.090	0.040–0.111	0.045–0.113	0.051–0.125	0.056–0.137	0.061–0.148	0.065–0.160
Average		0.131	0.122	0.112	0.103	0.093	0.084	0.075	0.067	0.06	0.054	0.051	0.051	0.053	0.055	0.058	0.066	0.072	0.08	0.087	0.095	0.101
SD		0.036	0.034	0.032	0.029	0.026	0.024	0.02	0.016	0.011	0.008	0.008	0.008	0.012	0.017	0.023	0.03	0.029	0.031	0.033	0.035	0.039
<i>Tensile</i>																						
Range		0.085–0.157	0.080–0.146	0.075–0.134	0.070–0.123	0.064–0.111	0.059–0.100	0.054–0.089	0.049–0.080	0.043–0.071	0.038–0.062	0.034–0.055	0.029–0.051	0.029–0.047	0.028–0.043	0.026–0.052	0.028–0.063	0.032–0.074	0.041–0.085	0.051–0.097	0.060–0.109	0.064–0.121
Average		0.122	0.113	0.104	0.095	0.086	0.077	0.069	0.061	0.054	0.048	0.043	0.039	0.037	0.036	0.036	0.038	0.047	0.058	0.069	0.080	0.090
SD		0.031	0.029	0.026	0.023	0.021	0.018	0.016	0.015	0.014	0.011	0.01	0.009	0.007	0.006	0.010	0.014	0.015	0.017	0.018	0.020	0.024

by the individual distribution of the stresses related to the curvature of the femur as well as its cervical-diaphyseal angle [21]. Models with significant varus deformation had higher tensile stresses at the end of the distal lateral diaphysis of the femur, which may indeed explain the mid-shaft diaphyseal location of some AFF. The models with the least axial deformation had increased tensile stresses in the proximal region, which may explain the occurrence of sub-trochanteric fractures. These observations are consistent with the study by Saita et al. [21], which evaluated the alignment of the lower limbs in standing position in 10 patients with AFF [22].

They found that the mechanical axes of the lower limbs, represented by the femoral-tibial angle (FTA), correlated with fracture height. Patients with medial-diaphyseal AFF had larger FTA (183.3°), while patients with sub-trochanterian AFF had smaller FTA (172.8°), concluding that the alignment of the lower limb affected the location of the fracture. In addition, the femoral morphological parameters reported in AFF populations in the Morin study [19] presented a wider alignment of varus at the knee joint relative to the control group (-1.6° (4.2) vs -0.4° (1.9)). Haider et al. [10] also attempted to determine the most important morphological parameters for AFF. They found that the greatest variations were caused by the radius of the femoral diaphysis and the angle of lateral curvature [20].

Our results therefore reinforce the idea that the abnormal mechanical properties of the femoral diaphysis may be due to misalignment of the lower limb and are associated with the development of AFF. Impairment of bone tissue properties, classified as minor criteria by ASBMR [23, 24] should also be considered.

Prolonged alteration of bisphosphonate-induced bone remodeling [25] or suppression of bone remodeling would result in deterioration of bone microarchitecture, reduce the bone repair process, and result in accumulation of bone micro-damage, source of low-energy diaphyseal femoral fractures or AFF [23]. An accurate estimation of fracture risk is therefore required before introduction of bisphosphonate therapy in osteoporotic patients [7, 26, 27]. For a long time, AFF was considered in terms of transverse stress fractures occurring in the lateral femoral diaphysis associated with increased bone fragility, itself associated with long-term anti-resorption therapy [2]. Meng Ai Png et al. [28] showed that bisphosphonate treatment was associated with periosteal femoral stress reaction called radiographic “black line”. An increased risk of AFF was observed in lateral cortical periosteal response, especially in cases of painful symptomatology [25, 29]. The pathophysiology of AFF is not yet fully understood. The fracture profiles and their different locations show

their multifactorial character. The combination of axial deformation stress and bone fragility create an environment conducive to the development of AFF.

The limitations of our FE modeling come from a small sample of patients whose original FTA we did not know about. Similarly, the applied boundary conditions did not take into account the specific weight of each subject. Stress distribution is directly related to the geometry and we have not varied the femoral geometry, even though variation can be the cause of the modification of the FTA, as is the case of curved femoral bone. Nor we did not consider the alteration of bone tissue in our model, but it remains a minor factor of AFF.

Conclusions

Variations in the mechanical axis of the lower limb influence stress distribution at the femur diaphysis and increase the risk of AFF. The axial deformation in varus is particularly at risk of AFF, whatever its origin: femoral, tibial; or femoral tibial deformity. Although the fracture profiles and their different locations show their multifactorial character, varus deformation seems to be a determining factor. The combination of axial deformation stresses and bone fragility consequently contribute to the creation of an environment favorable to the development of AFF.

Authors' contributions

DB: study design and protocol. MS: redaction. KA: statistical analysis and study protocol. AB: reviewing and corrections. AG: corrections and statistical analysis. TV: head of laboratory and study protocol. All authors read and approved the final manuscript.

Funding

No funding sources.

Availability of data and materials

Not applicable.

Declarations

Ethics approval and consent to participate

Not applicable.

Consent for publication

All authors consent for publication.

Competing interests

No competing interests.

Author details

¹Department of Orthopaedic Surgery and Traumatology, Hôpital Pierre Zobda Quitman, University Hospital, 97261 Fort-de-France Cedex, Martinique, France.

²Institute Pprime UPR 3346, CNRS – University of Poitiers – ISAE-ENSMA,

Poitiers, France. ³Department of Mechanical Engineering, Faculty of Technology Sciences, University of Mentouri Brothers Constantine, Ain-El-Bey Way, P.O. Box 325, 25017 Constantine, Algeria.

Received: 24 January 2022 Accepted: 9 March 2022
Published online: 15 March 2022

References

- Shane E, Burr D, Ebeling PR, Abrahamsen B, Adler RA, Brown TD, et al. Atypical subtrochanteric and diaphyseal femoral fractures: report of a task force of the American Society for Bone and Mineral Research. *J Bone Miner Res*. 2010;25:2267–94.
- Shane E, Burr D, Abrahamsen B, Adler RA, Brown TD, Cheung AM, et al. Atypical subtrochanteric and diaphyseal femoral fractures: second report of a task force of the American Society for Bone and Mineral Research. *J Bone Miner Res*. 2014;29:1–23.
- Thompson RN, Armstrong CL, Heyburn G. Bilateral atypical femoral fractures in a patient prescribed denosumab - a case report. *Bone*. 2014;61:44–7.
- Mahjoub Z, Jean S, Leclerc J-T, Brown JP, Boulet D, Pelet S, et al. Incidence and characteristics of atypical femoral fractures: clinical and geometrical data. *J Bone Miner Res*. 2016;31:767–76.
- Meier RPH, Perneger TV, Stern R, Rizzoli R, Peter RE. Increasing occurrence of atypical femoral fractures associated with bisphosphonate use. *Arch Intern Med*. 2012;172:930–6.
- Lo JC, Huang SY, Lee GA, Khandelwal S, Khandewal S, Provus J, et al. Clinical correlates of atypical femoral fracture. *Bone*. 2012;51:181–4.
- Giusti A, Hamdy NAT, Dekkers OM, Ramautar SR, Dijkstra S, Papapoulos SE. Atypical fractures and bisphosphonate therapy: a cohort study of patients with femoral fracture with radiographic adjudication of fracture site and features. *Bone*. 2011;48:966–71.
- Sasaki S, Miyakoshi N, Hongo M, Kasukawa Y, Shimada Y. Low-energy diaphyseal femoral fractures associated with bisphosphonate use and severe curved femur: a case series. *J Bone Miner Metab*. 2012;30:561–7.
- Oh Y, Wakabayashi Y, Kurosa Y, Fujita K, Okawa A. Potential pathogenic mechanism for stress fractures of the bowed femoral shaft in the elderly: Mechanical analysis by the CT-based finite element method. *Injury*. 2014;45:1764–71.
- Haider IT, Schneider P, Michalski A, Edwards WB. Influence of geometry on proximal femoral shaft strains: Implications for atypical femoral fracture. *Bone*. 2018;110:295–303.
- Hagen JE, Miller AN, Ott SM, Gardner M, Morshed S, Jeray K, et al. Association of atypical femoral fractures with bisphosphonate use by patients with varus hip geometry. *J Bone Joint Surg Am*. 2014;96:1905–9.
- Tano A, Oh Y, Fukushima K, Kurosa Y, Wakabayashi Y, Fujita K, et al. Potential bone fragility of mid-shaft atypical femoral fracture: Biomechanical analysis by a CT-based nonlinear finite element method. *Injury*. 2019;50:1876–82.
- Ali AA, Cristofolini L, Schileo E, Hu H, Taddei F, Kim RH, et al. Specimen-specific modeling of hip fracture pattern and repair. *J Biomech*. 2014;47:536–43.
- Grassi L, Väänänen SP, Ristinmaa M, Jurvelin JS, Isaksson H. How accurately can subject-specific finite element models predict strains and strength of human femora? Invest Using Full-Field Meas *J Biomech*. 2016;49:802–6.
- Hambli R, Allaoui S. A robust 3D finite element simulation of human proximal femur progressive fracture under stance load with experimental validation. *Ann Biomed Eng*. 2013;41:2515–27.
- Schileo E, Dall'ara E, Taddei F, Malandrino A, Schotkamp T, Baleani M, et al. An accurate estimation of bone density improves the accuracy of subject-specific finite element models. *J Biomech*. 2008;41:2483–91.
- Morgan EF, Bayraktar HH, Keaveny TM. Trabecular bone modulus-density relationships depend on anatomic site. *J Biomech*. 2003;36:897–904.
- Subburaj K, Ravi B, Agarwal M. Computer-aided methods for assessing lower limb deformities in orthopaedic surgery planning. *Comput Med Imaging Graph*. 2010;34:277–88.
- Kheirollahi H, Luo Y. Assessment of hip fracture risk using cross-section strain energy determined by QCT-based finite element modeling. *Biomed Res Int*. 2015;2015:413839.
- Morin SN, Wall M, Belzile EL, Godbout B, Moser TP, Michou L, et al. Assessment of femur geometrical parameters using EOS™ imaging technology in patients with atypical femur fractures; preliminary results. *Bone*. 2016;83:184–9.
- Oh Y, Fujita K, Wakabayashi Y, Kurosa Y, Okawa A. Location of atypical femoral fracture can be determined by tensile stress distribution influenced by femoral bowing and neck-shaft angle: a CT-based nonlinear finite element analysis model for the assessment of femoral shaft loading stress. *Injury*. 2017;48:2736–43.
- Saita Y, Ishijima M, Mogami A, Kubota M, Baba T, Kaketa T, et al. The fracture sites of atypical femoral fractures are associated with the weight-bearing lower limb alignment. *Bone*. 2014;66:105–10.
- Abrahamsen B, Eiken P, Eastell R. Subtrochanteric and diaphyseal femur fractures in patients treated with alendronate: a register-based national cohort study. *J Bone Miner Res*. 2009;24:1095–102.
- Donnelly E, Meredith DS, Nguyen JT, Gladnick BP, Rebolledo BJ, Shaffer AD, et al. Reduced cortical bone compositional heterogeneity with bisphosphonate treatment in postmenopausal women with intertrochanteric and subtrochanteric fractures. *J Bone Miner Res*. 2012;27:672–8.
- Isaacs JD, Shidiak L, Harris IA, Szomor ZL. Femoral insufficiency fractures associated with prolonged bisphosphonate therapy. *Clin Orthop Relat Res*. 2010;468:3384–92.
- Gong H, Zhang M, Fan Y, Kwok WL, Leung PC. Relationships between femoral strength evaluated by nonlinear finite element analysis and BMD, material distribution and geometric morphology. *Ann Biomed Eng*. 2012;40:1575–85.
- Kanis JA, McCloskey EV, Johansson H, Oden A, Melton LJ, Khaltaev N. A reference standard for the description of osteoporosis. *Bone*. 2008;42:467–75.
- Png MA, Koh JSB, Goh SK, Fook-Chong S, Howe TS. Bisphosphonate-related femoral periosteal stress reactions: scoring system based on radiographic and MRI findings. *AJR Am J Roentgenol*. 2012;198:869–77.
- Schilcher J, Aspenberg P. Incidence of stress fractures of the femoral shaft in women treated with bisphosphonate. *Acta Orthop*. 2009;80:413–5.

Publisher's Note

Springer Nature remains neutral with regard to jurisdictional claims in published maps and institutional affiliations.

Ready to submit your research? Choose BMC and benefit from:

- fast, convenient online submission
- thorough peer review by experienced researchers in your field
- rapid publication on acceptance
- support for research data, including large and complex data types
- gold Open Access which fosters wider collaboration and increased citations
- maximum visibility for your research: over 100M website views per year

At BMC, research is always in progress.

Learn more biomedcentral.com/submissions

